Supporting Information for

Spatial- and temporal-pattern of global soil heterotrophic respiration in terrestrial ecosystems

Xiaolu Tang[1, 2], Shaohui Fan[3], Manyi Du[4], Wenjie Zhang[5, 6], Sicong Gao[6], Shibing Liu[1], Guo Chen[1], Zhen Yu[7], Yitong Yao[8], Wunian Yang[1]

[1]College of Earth Science, Chengdu University of Technology, Chengdu, Sichuan, P.R. China
[2]State Environmental Protection Key Laboratory of Synergetic Control and Joint Remediation for Soil & Water Pollution, Chengdu University of Technology, Chengdu, P. R. China
[3]Key laboratory of Bamboo and Rattan, International Centre for Bamboo and Rattan, Beijing, P.R. China
[4]Experimental Center of Forestry in North China, Chinese Academy of Forestry, Beijing, China
[5]State Key Laboratory of Resources and Environmental Information System, Institute of Geographic Sciences and Natural Resources Research, Beijing, China
[6]School of Life Science, University of Technology Sydney, NSW, Australia
[7]Department of Ecology, Evolution, and Organismal Biology, Iowa State University, Ames, IA, USA
[8]Sino-French Institute for Earth System Science, College of Urban and Environmental Sciences, Peking University, Beijing, P.R. China

Corresponding authors: Shaohui Fan (fansh@icbr.ac.cn) ; Wunian Yang (ywn@cdut.edu.cn)

Contents of this file

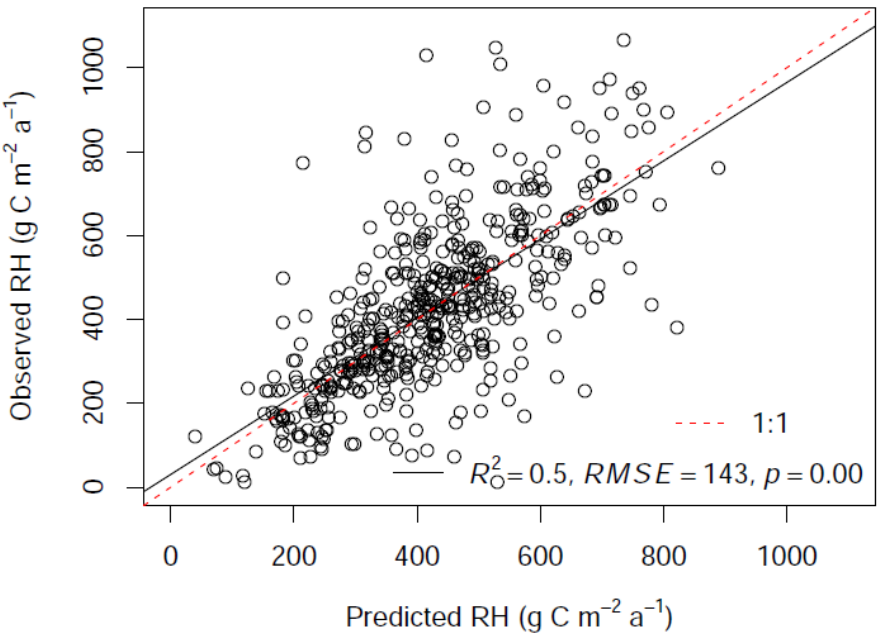

Figure S1. Comparison of observed soil heterotrophic respiration (RH) and predicted RH from Random Forest by 10-fold cross-validation.

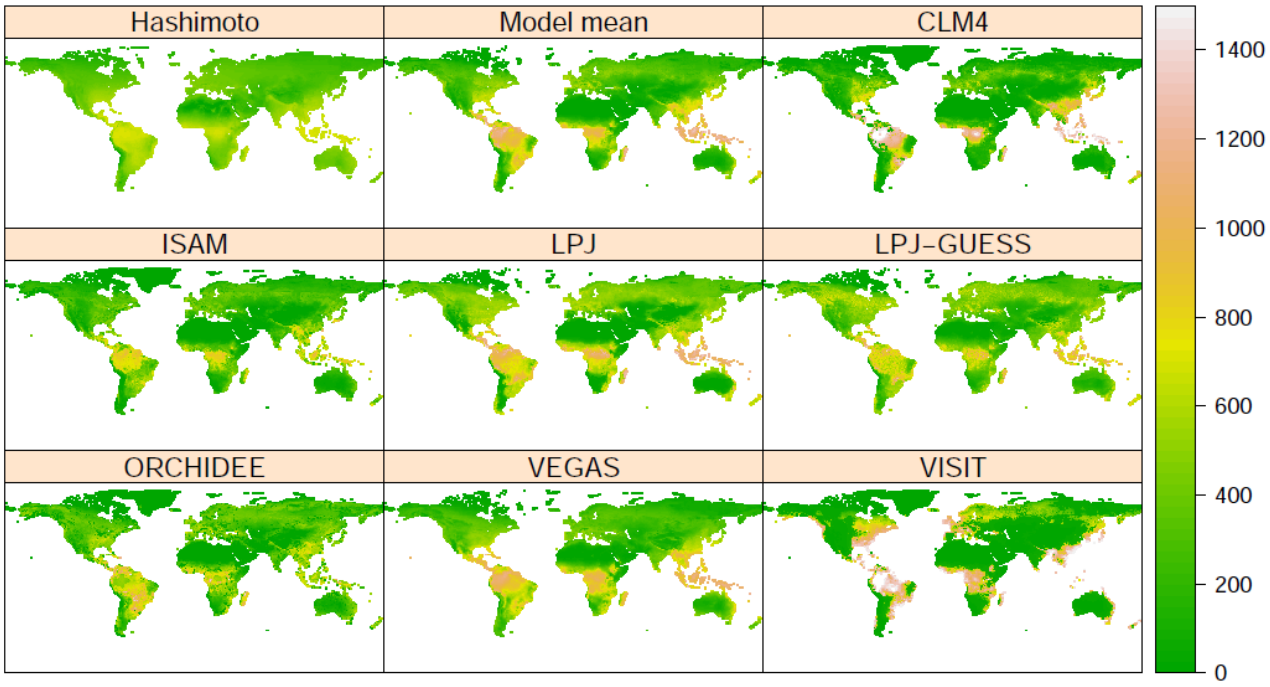

Figure S2. Spatial distribution for TRENDY/Hashimoto RH over 1981-2010

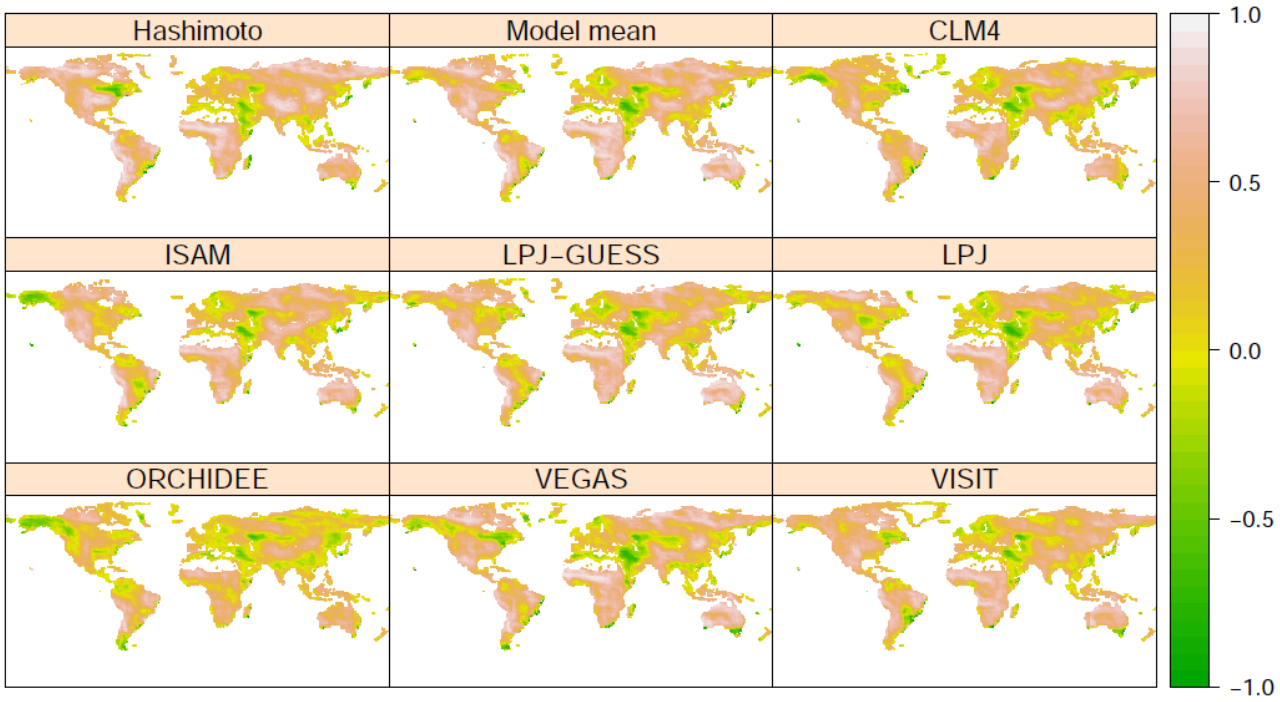

Figure S3. Cross-correlation between data-derived RH and TRENDY/Hashimoto RH

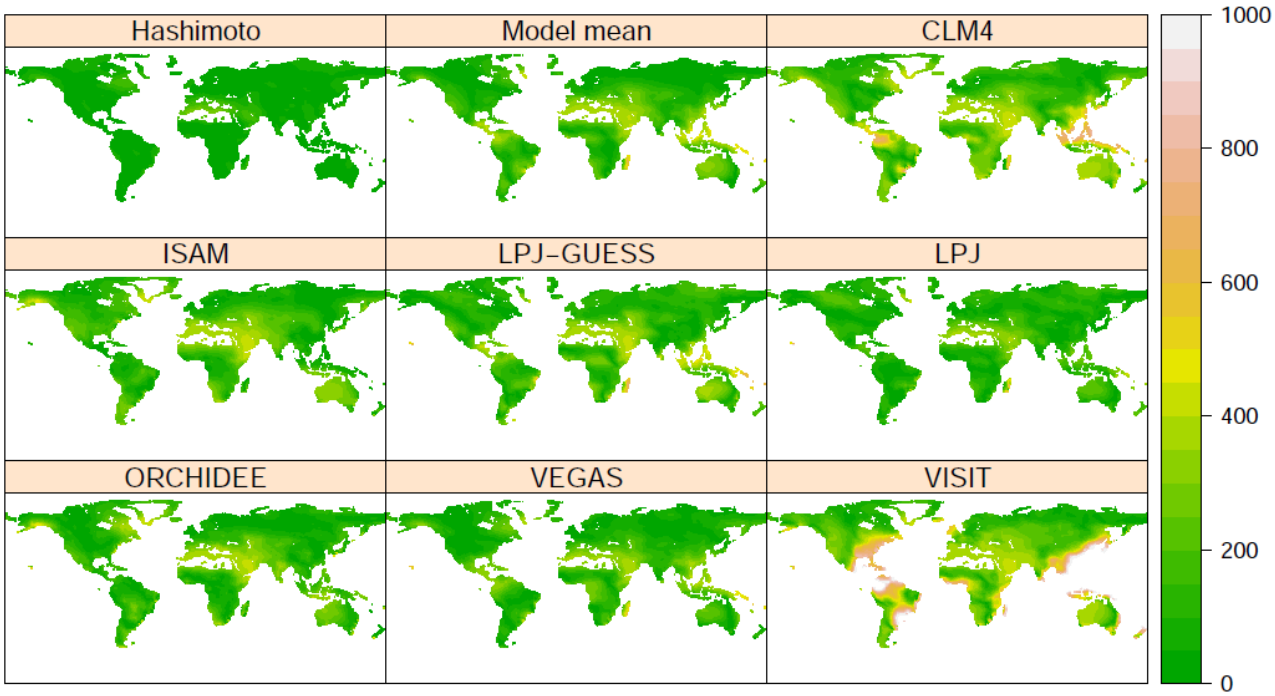

Figure S4. Absolute distance between data-derived RH and TRENDY/Hashimoto RH

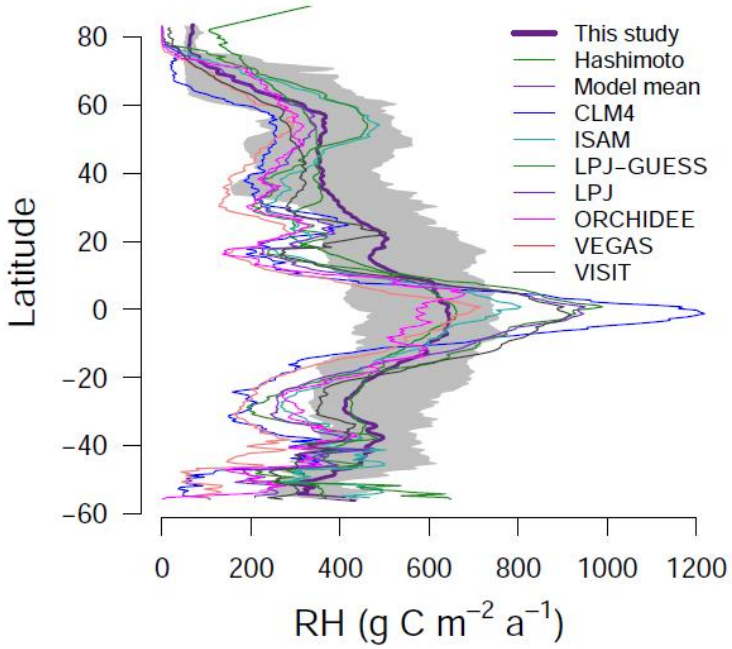

Figure S5. Latitudinal gradient of RH for data-derived product and TRENDY models. The grey range means 2.5 to 97.5 percentile ranges of the data-derived RH in this study.

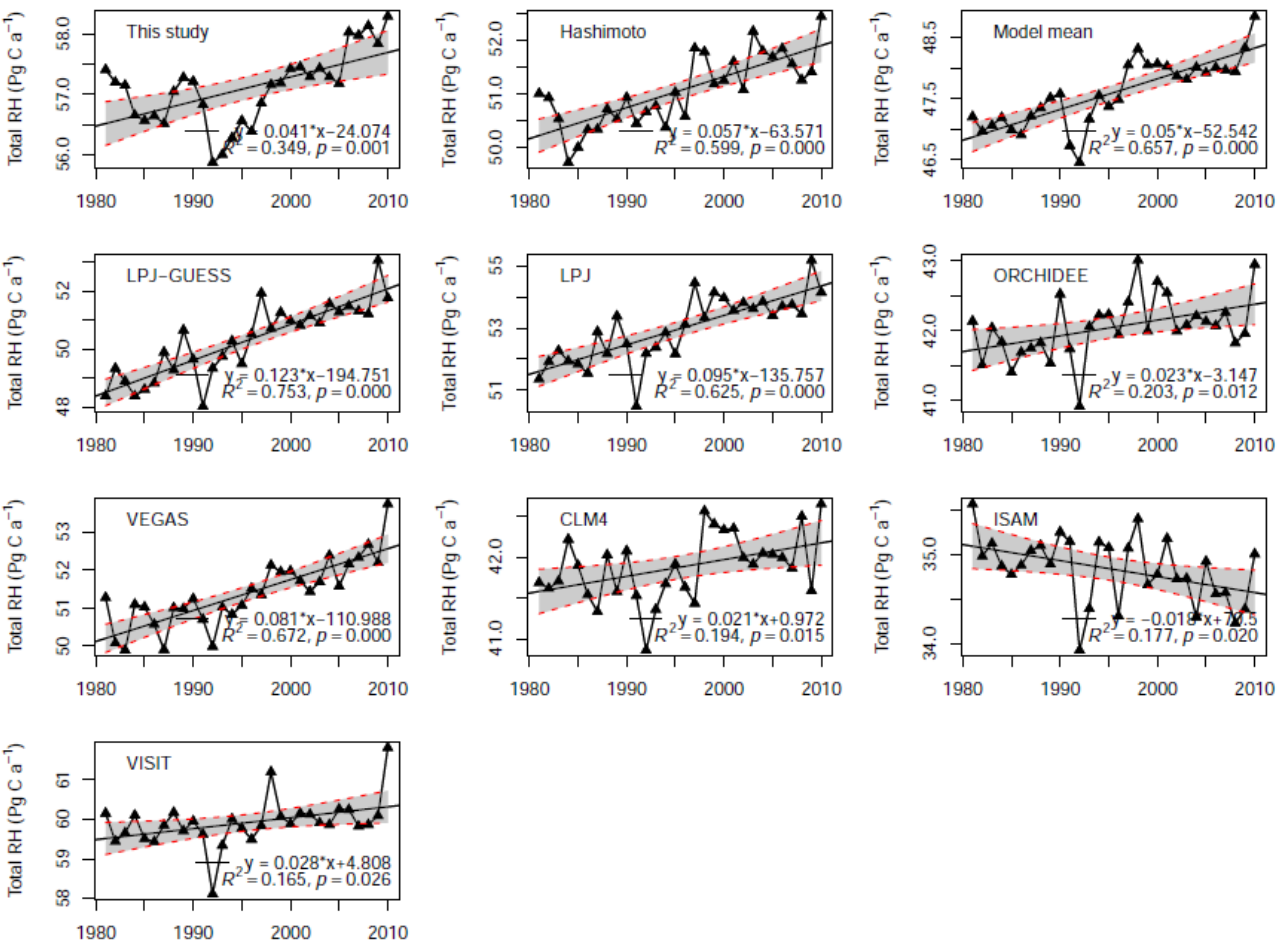

Figure S6. Temporal change of data-derived and TRENDY/Hashimoto RH from 1980 to 2010. The grey area indicates 95% confidence intervals.

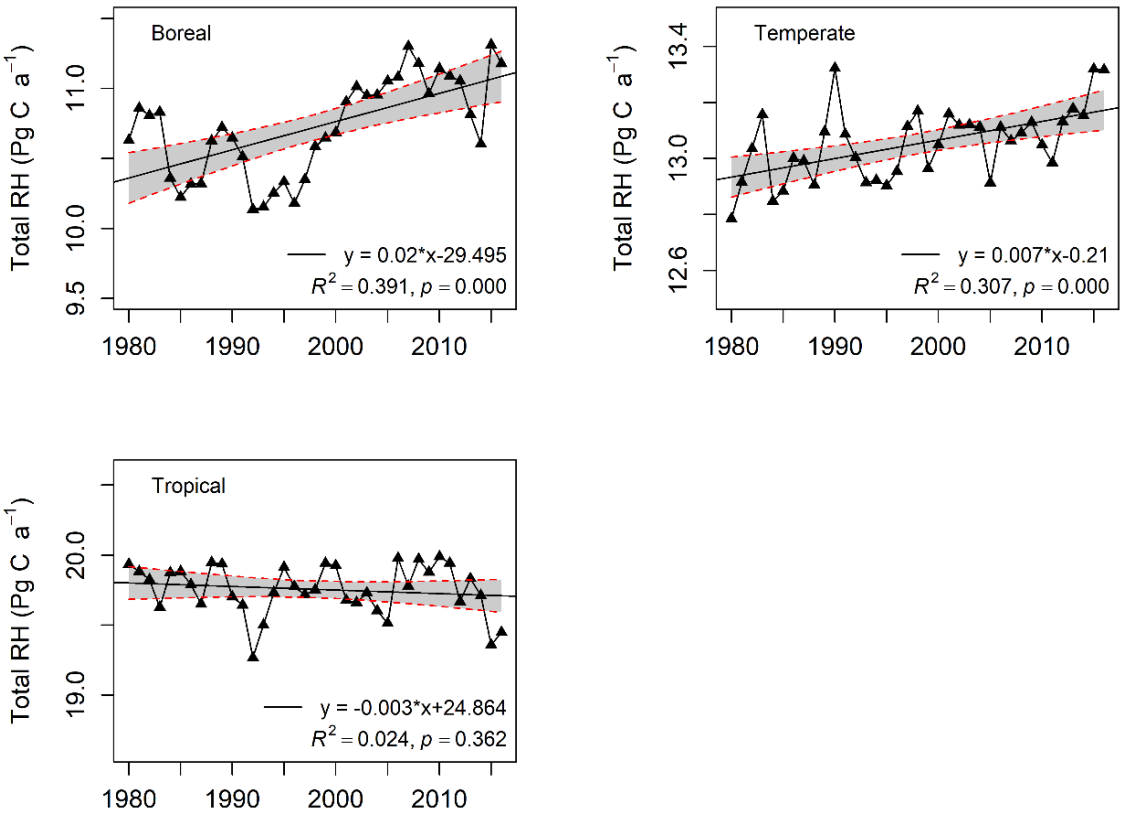

Figure S7. Annual change of data-derived RH for boreal, temperate and tropical areas from 1980 to 2016. The grey area indicates 95% confidence intervals.

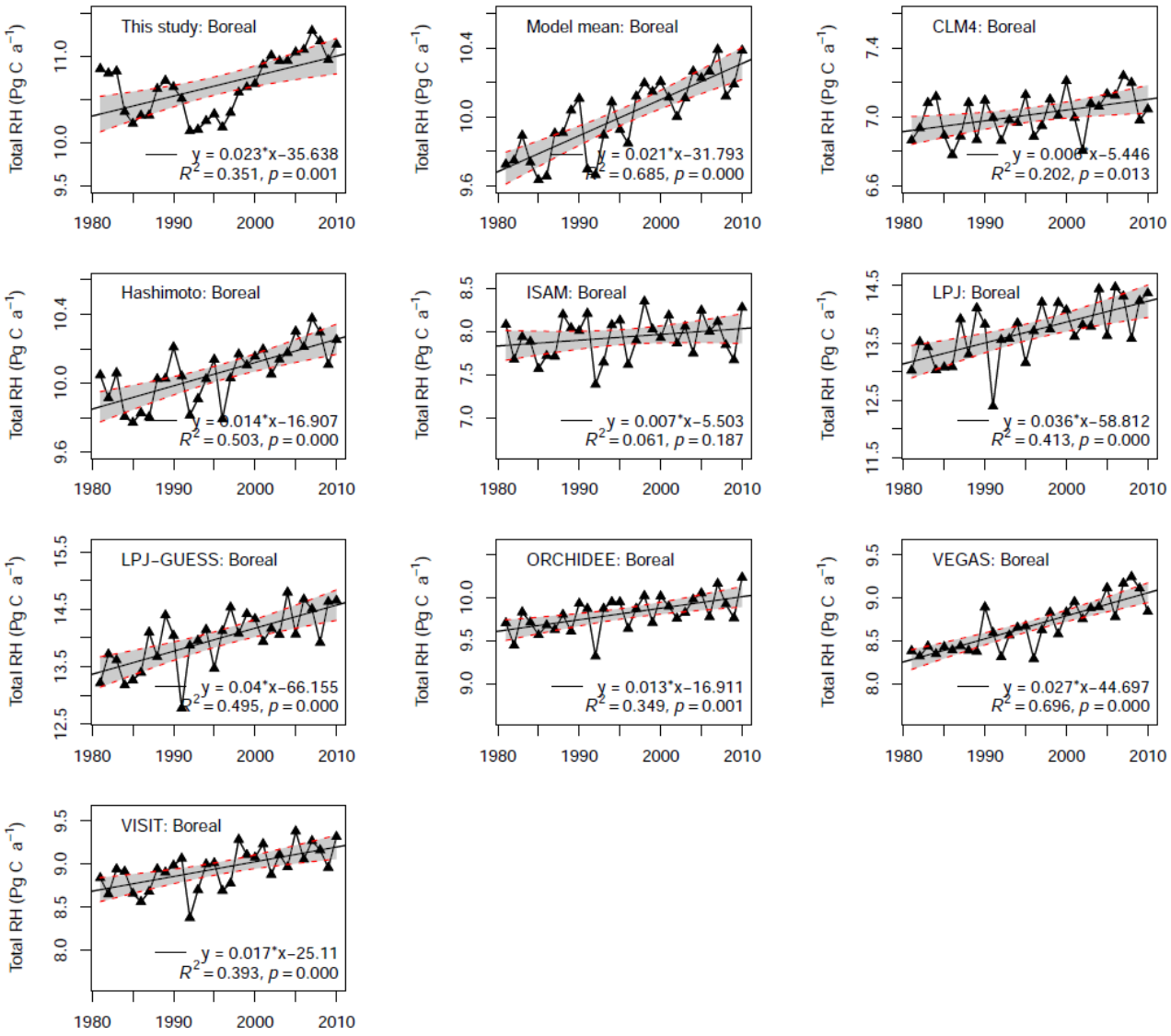

Figure S8. Annual change of TRENDY/Hashimoto RH for boreal areas. The grey area indicates 95% confidence intervals.

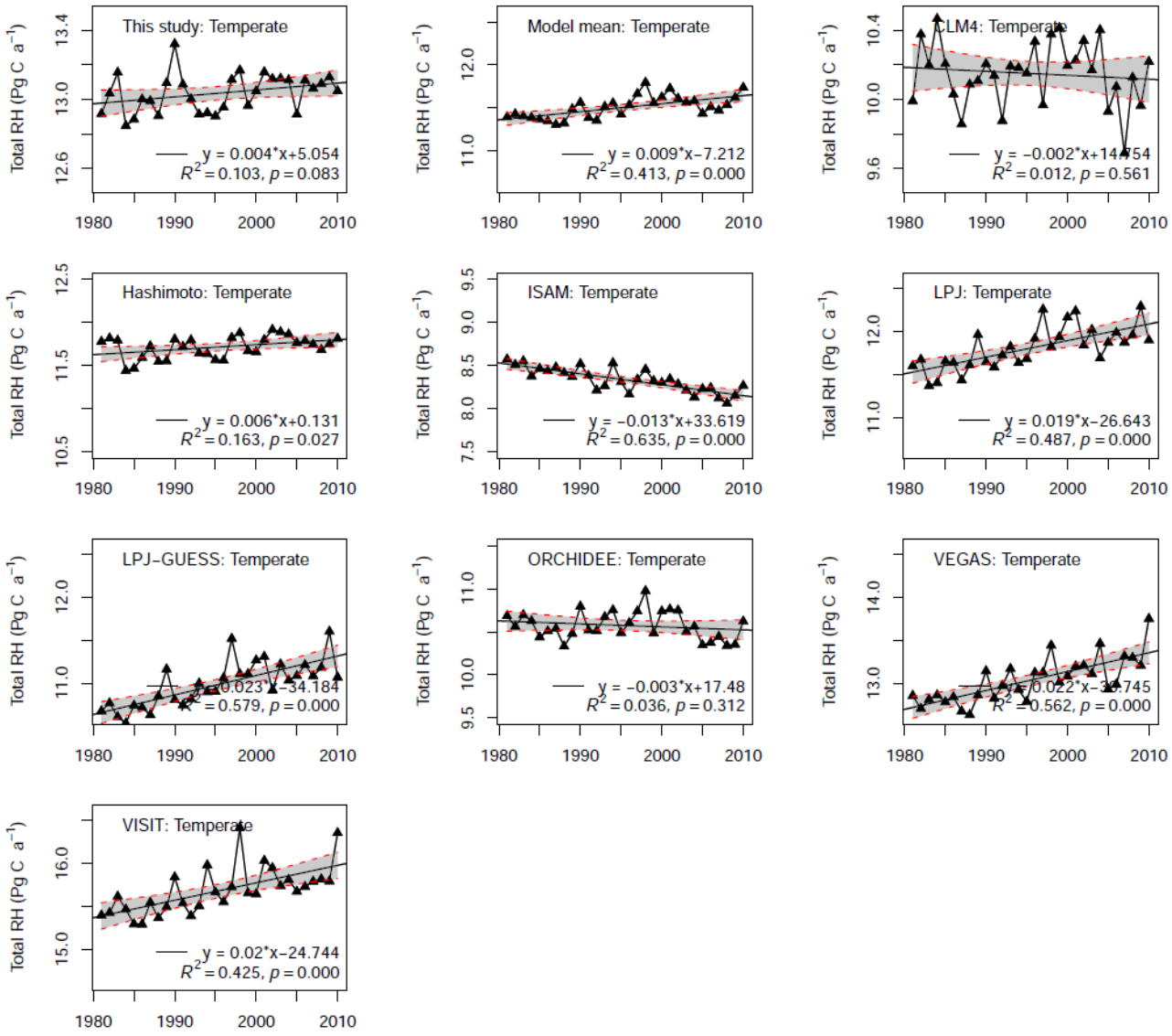

Figure S9. Annual change of TRENDY/Hashimoto RH for temperate areas. The grey area indicates 95% confidence intervals.

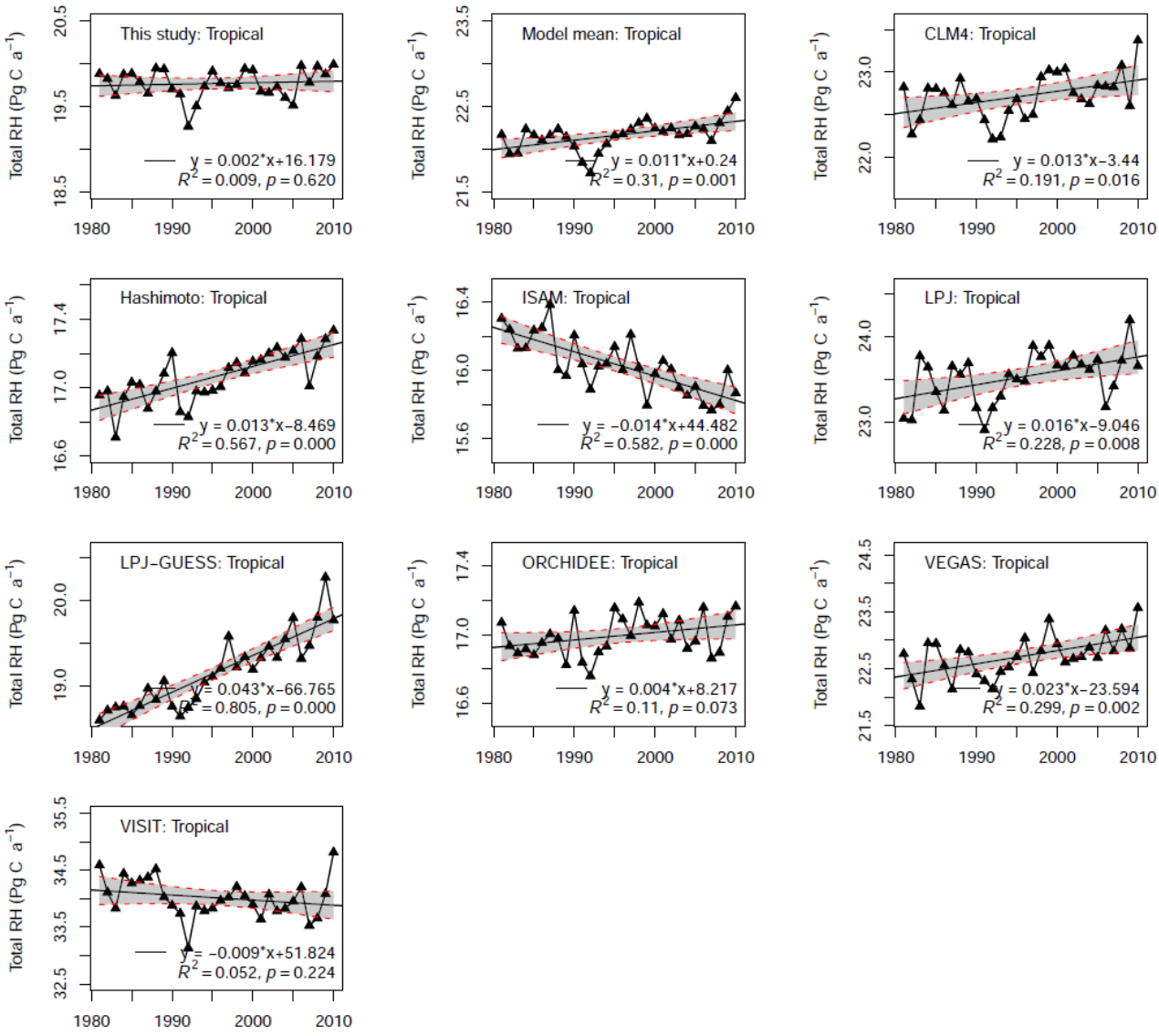

Figure S10. Annual change of TRENDY/Hashimoto RH for tropical areas. The grey area indicates 95% confidence intervals.

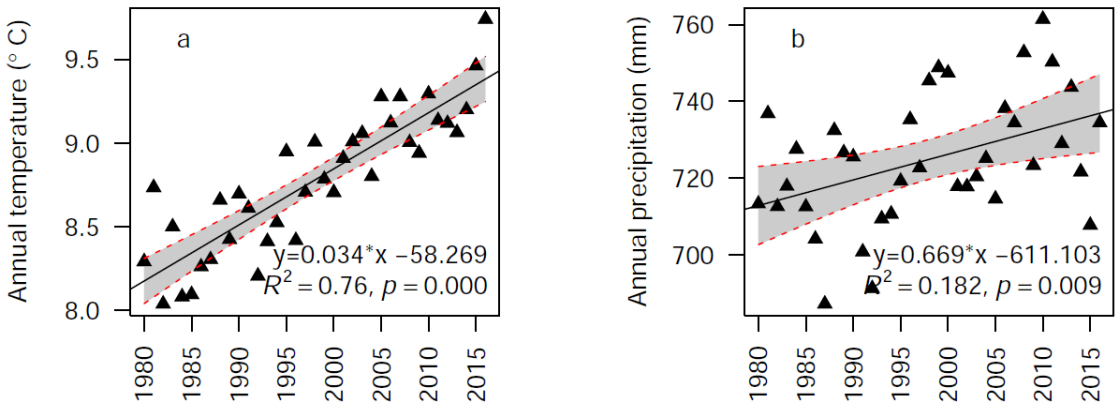

Figure S11. Temporal change of (a) global mean annual temperature, (b) precipitation. The grey area indicates 95% confidence intervals

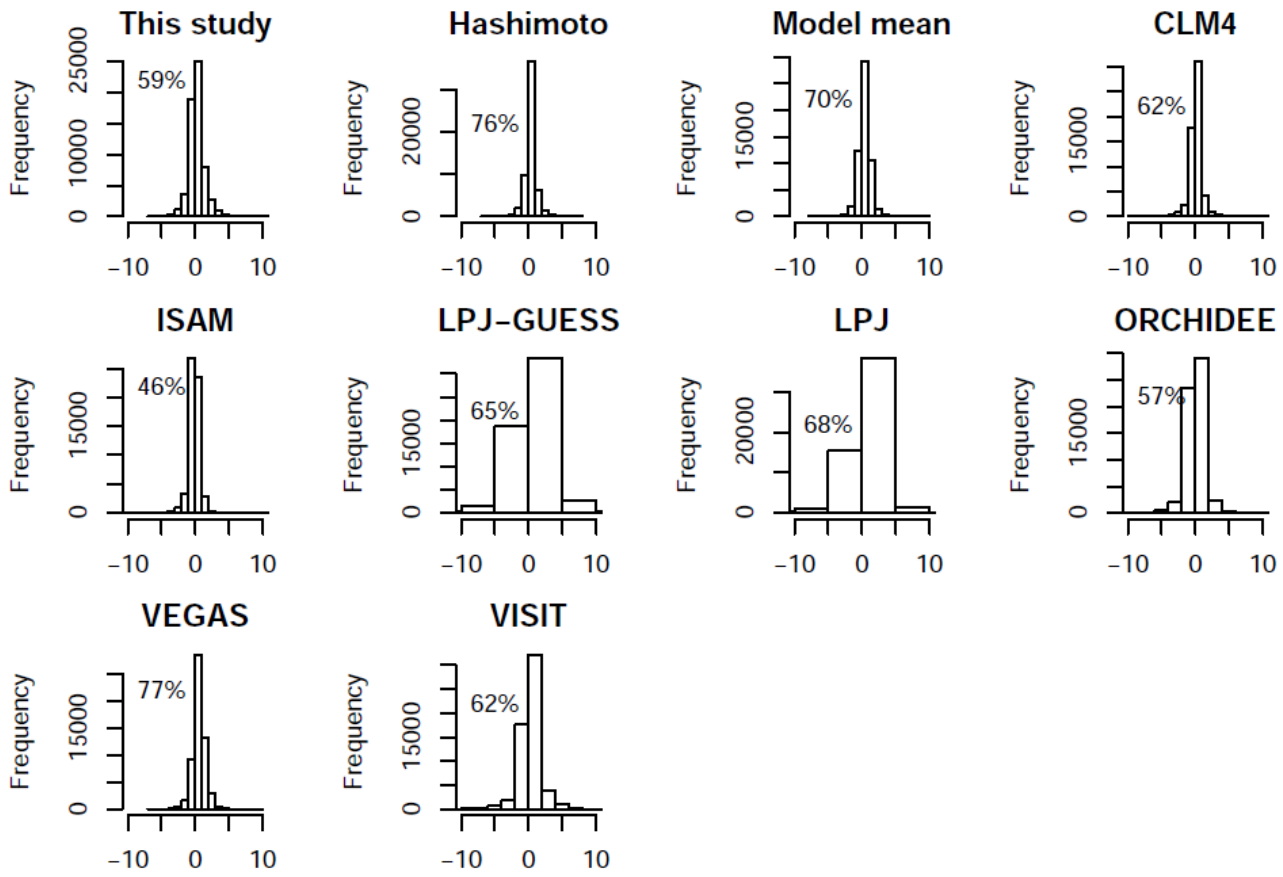

Figure S12. Frequency of temporal trend of data-derived RH, TRENDY/Hashimoto models. The percentages on the Figure indicated the increasing areas of RH within 1981-2010 for data-derived RH, Hashimoto, model mean and seven trendy models, respectively

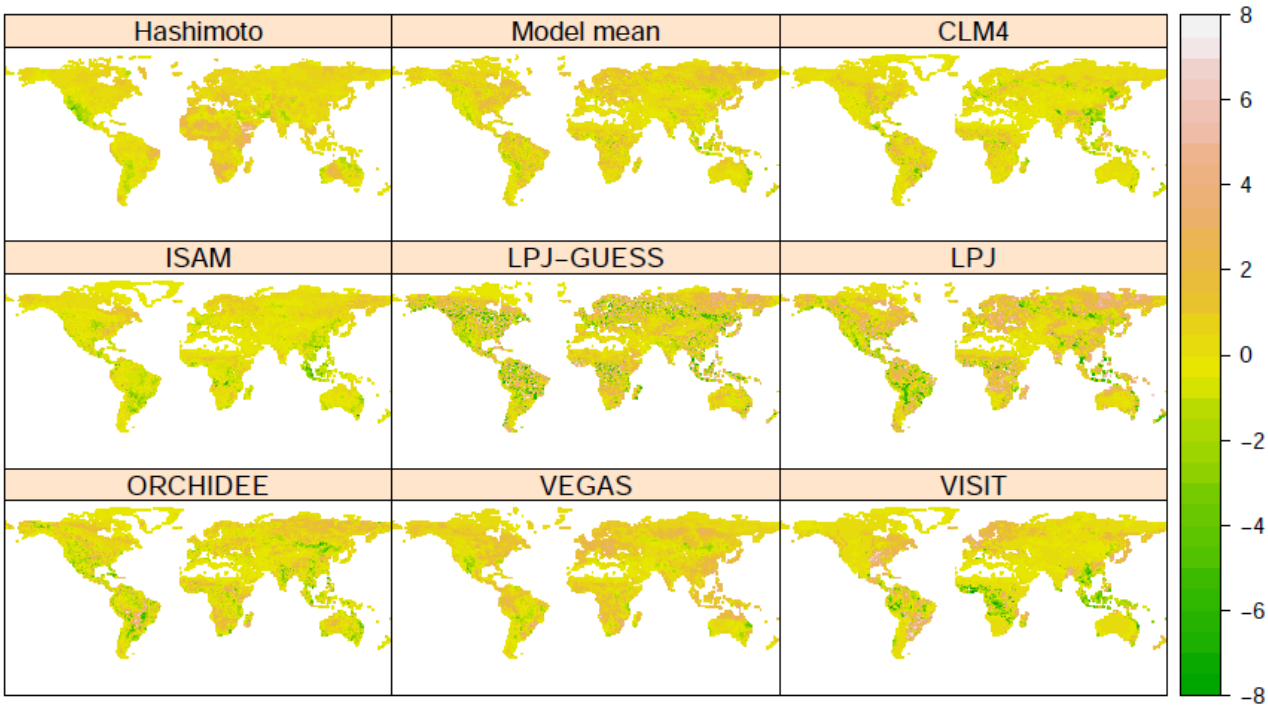

Figure S13. Spatial pattern in the trend of RH for TRENDY/Hashimoto models

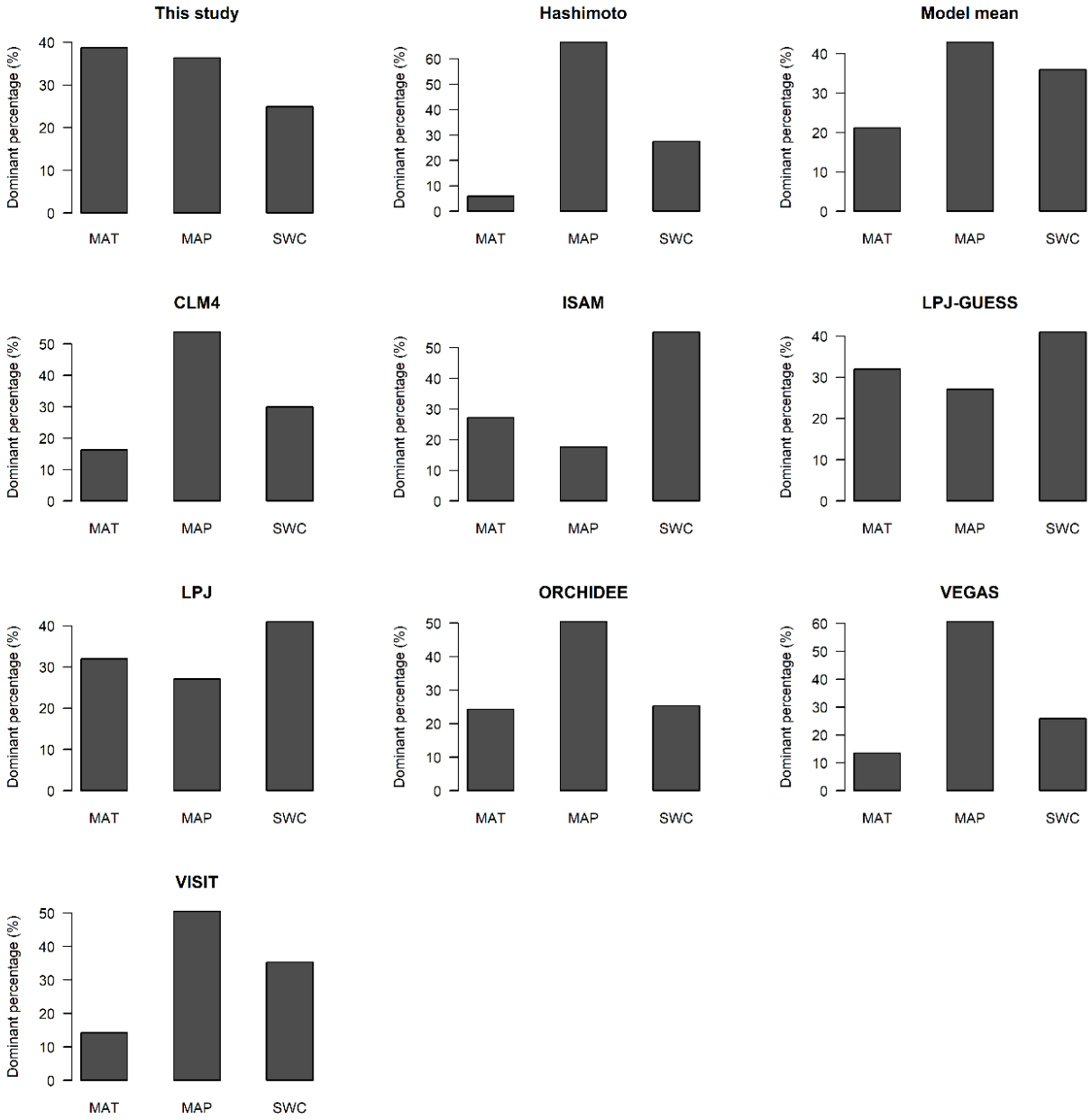

Figure S14. The percentage of areas dominated by temperature, precipitation and soil water content for Hashimoto/TRENDY RH

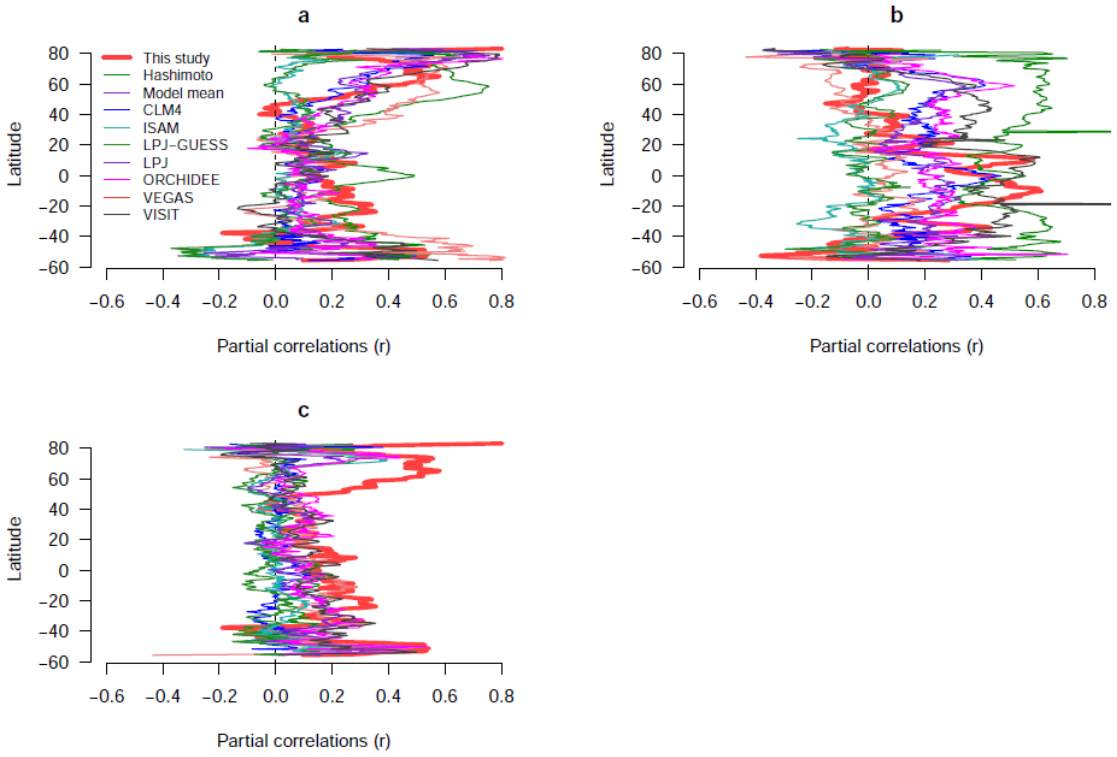

Figure S15. Latitudinal gradients of partial correlation coefficient between RH and (a) temperature, (b) precipitation and (c) soil water content. When analyzing the partial correlation between RH and the proxy, the other two proxies were controlled.

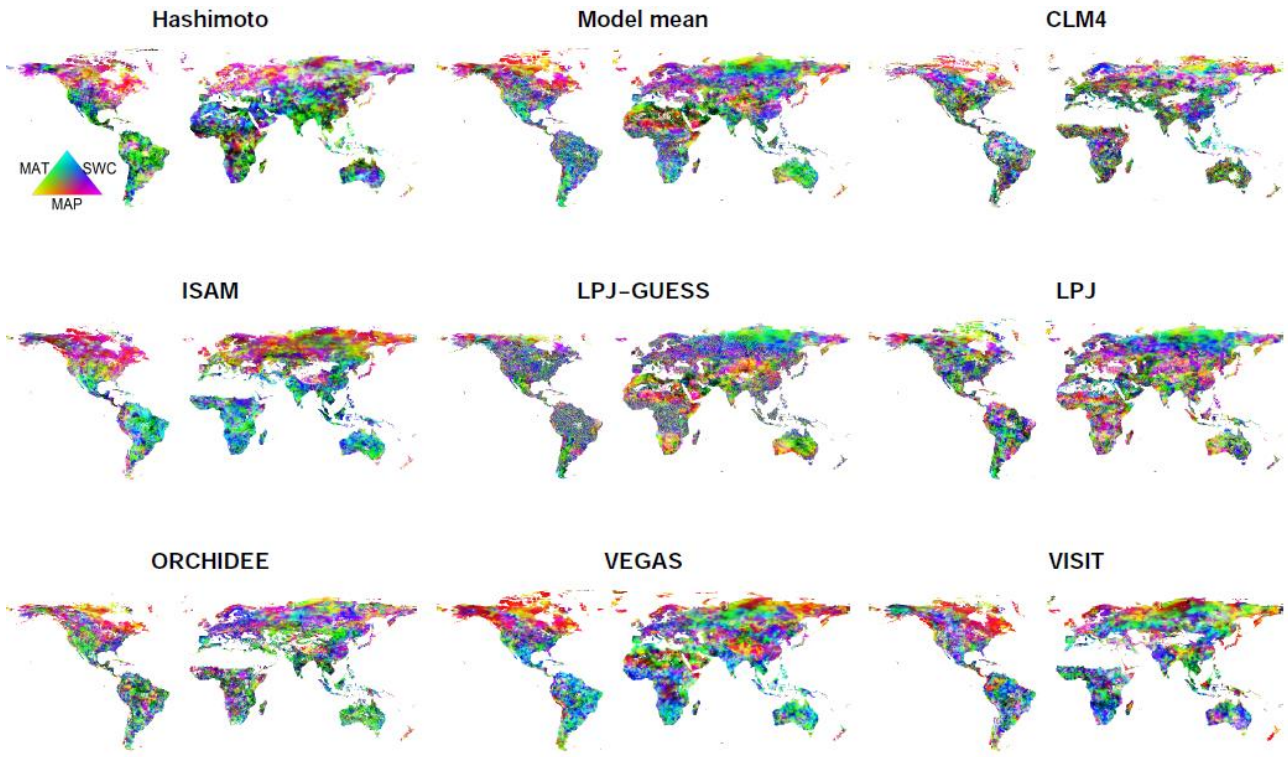

Figure S16. Environmental drivers for TRENDY/Hashimoto RH. MAT = mean annual temperature, MAP = mean annual precipitation, SWC = soil water content

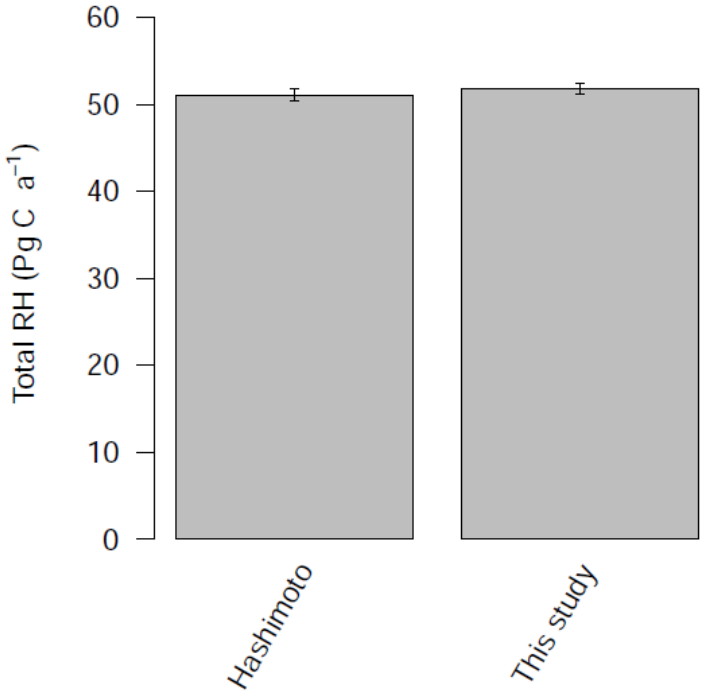

Figure S17. Global Hashimoto RH and data-derived RH in this study masked by Hashimoto RH. After masked for same land area, RH was 51.1 Pg C a^{-1} for Hashimoto and 51.8 Pg C a^{-1} for this study. The error bar means the standard deviation.

Table S1. Global variables used for predicting the temporal and spatial RH

	Variables	Type	Type of variability	Sources
Climate	Mean annual temperature	Split	Yearly	https://crudata.uea.ac.uk/cru/data/hrg/cru_ts_4.01/ (Harris et al., 2014)
	Mean annual precipitation	Split	Yearly	
	Diurnal temperature range	Split	Yearly	
	Nitrogen deposition	Split	Yearly	https://www.isimip.org/gettingstarted/availability-input-data-isimip2b/ (Lamarque et al., 2013)
	Palmer Drought Severity Index	Split	Yearly	https://www.esrl.noaa.gov/psd/data/gridded/data.pdsi.html (Dai et al., 2004)
	Shortwave radiation	Split	Yearly	https://www.esrl.noaa.gov (Kalnay et al., 1996)
Soil	Soil carbon content	-	Static	https://soilgrids.org/#!/?layer=TAXNWRB_250m (Hengl et al., 2017)
	Soil nitrogen content	-	Static	https://webmap.ornl.gov/ogc/index.jsp (Global Soil Data, 2000)
	Soil water content	Split	Yearly	https://www.esrl.noaa.gov/psd/data/gridded/data.cpcsoil.html (van den Dool et al., 2003)

References

Dai, A., Trenberth, K. E., and Qian, T.: A Global Dataset of Palmer Drought Severity Index for 1870–2002: Relationship with Soil Moisture and Effects of Surface Warming, Journal of Hydrometeorology, 5, 1117-1130, http://dx.doi.org/10.1175/JHM-386.1, 2004.

Global Soil Data, T.: Global Gridded Surfaces of Selected Soil Characteristics (IGBP-DIS). ORNL Distributed Active Archive Center, http://dx.doi.org/10.3334/ornldaac/569, 2000.

Harris, I., Jones, P., Osborn, T., and Lister, D.: Updated high‐resolution grids of monthly climatic observations–the CRU TS3. 10 Dataset, Int. J. Climatol., 34, 623-642, http://dx.doi.org/10.1002/joc.3711, 2014.

Hengl, T., Mendes de Jesus, J., Heuvelink, G. B., Ruiperez Gonzalez, M., Kilibarda, M., Blagotic, A., Shangguan, W., Wright, M. N., Geng, X., Bauer-Marschallinger, B., Guevara, M. A., Vargas, R., MacMillan, R. A., Batjes, N. H., Leenaars, J. G., Ribeiro, E., Wheeler, I., Mantel, S., and Kempen, B.: SoilGrids250m: Global gridded soil information based on machine learning, PLoS One, 12, e0169748, http://dx.doi.org/10.1371/journal.pone.0169748, 2017.

Kalnay, E., Kanamitsu, M., Kistler, R., Collins, W., Deaven, D., Gandin, L., Iredell, M., Saha, S., White, G., Woollen, J., Zhu, Y., Chelliah, M., Ebisuzaki, W., Higgins, W., Janowiak, J., Mo, K. C., Ropelewski, C., Wang, J., Leetmaa, A., Reynolds, R., Jenne, R., and Joseph, D.: The NCEP/NCAR 40-year reanalysis project, Bull. Am. Meteorol. Soc., 77, 437-471, http://dx.doi.org/10.1175/1520-0477(1996)077<0437:Tnyrp>2.0.Co;2, 1996.

Lamarque, J. F., Dentener, F., McConnell, J., Ro, C. U., Shaw, M., Vet, R., Bergmann, D., Cameron-Smith, P., Dalsoren, S., Doherty, R., Faluvegi, G., Ghan, S. J., Josse, B., Lee, Y. H., MacKenzie, I. A., Plummer, D., Shindell, D. T., Skeie, R. B., Stevenson, D. S., Strode, S., Zeng, G., Curran, M., Dahl-Jensen, D., Das, S., Fritzsche, D., and Nolan, M.: Multi-model mean nitrogen and sulfur deposition from the Atmospheric Chemistry and Climate Model Intercomparison Project (ACCMIP): evaluation of historical and projected future changes, Atmos. Chem. Phys., 13, 7997-8018, http://dx.doi.org/10.5194/acp-13-7997-2013, 2013.

van den Dool, H., Huang, J., and Fan, Y.: Performance and analysis of the constructed analogue method applied to U.S. soil moisture over 1981–2001, J. Geophys. Res. Atmos., 108, http://dx.doi.org/10.1029/2002jd003114, 2003.